

SAR Imagery-Based Detection to Support Inundated Observation Using Web Technology

P. Limlahapun and H. Fukui

Abstract—Inundated monitoring using satellite-based images can be successively performed independently of weather conditions, especially on synthetic aperture radar (SAR) images. This capability is used to perform flood observation on tracks. However, the operation of image detection requires practical skills in dealing with image processing tools and theoretical applications on signal penetration of the electromagnetic spectrum region. In this paper, we propose a method and algorithm suitable for detecting water features on satellite images through a web interface. This approach helps provide inundated features as auxiliary information to rapidly support flood management. In addition, it serves as an option for general public use. While SAR images remain difficult to interpret, the proposed system aids in quickly detecting inundated areas compared to the image processing software. Furthermore, it is not limited to area-based calculations, which can be applied worldwide.

Index Terms—Feature detection, inundated area, SAR imagery, web-based system.

I. INTRODUCTION

Satellite-based imagery is a valuable data resource, particularly in crisis situations. For example, the Nepal earthquake of April 25, 2015 was closely followed by a second quake on May 12, while the volcano on Kuchinoerabu Island in Yakushima of southern Japan erupted close thereafter on May 29, 2015. Space agencies in many countries provided high-resolution images for government institutions and other organizations to assess the damaged areas. This information helped guide these organizations in conducting evacuations and relief plans, and in assisting far-reaching affected areas. The freely available Moderate Resolution Imaging Spectroradiometer (MODIS), which has 250 m, 500 m, and 1 km spatial resolutions, was provided online. In addition, a US government agency freely provided Landsat 28-m spatial resolution images to users. Nevertheless, both MODIS and Landsat images are derived from optical or multispectral sensors, which have some limitations, primarily in terms of cloud penetration. In the case of the rainy season, which typically leads to flooding periods, image products from synthetic aperture radar (SAR) sensors of areas that can be imaged without weather, seasonal, day, or night constraints may be a viable alternative.

Flood mapping information is required in flood-prone areas to help in preparations, evacuations, and receiving of disaster assistance. Remote sensing technology overcomes

conventional techniques (e.g., surveys) with budget, distance, time, and the influence of unknown factors in assessing wide spaces on earth. Radar imagery has become a focus of studies of remote sensing applications, whose multi-resolution and coverage capabilities provide significant flexibility and supportive approaches to earth observation. Accordingly, in this paper, we propose algorithms to extract water features from SAR imagery through web technology. The proposed system platform focuses on data browsing, step-wise processing, and output visualization in a user-friendly manner.

II. THEORETICAL BACKGROUND AND RELATED WORKS

Flood extent mapping provides a spatially-based approximation of flooding effects. Information extracted from remote sensing imagery can be a valuable asset for disaster relief teams to conduct rescue plans or assist people in affected zones. Remote sensing (RS) is defined as the acquisition of information of an object or phenomenon using a device (in an aircraft, spacecraft, or ship) without physical contact with the object [1]. RS technology has been used in many fields of study (e.g., communications, resource management, disaster response), and it covers various environments (e.g., atmospheric, surface, ocean). RS image products are obtained from effective information sources where interest areas are inaccessible. Radio detection and ranging (RADAR) operates in the microwave portion of the electromagnetic spectrum (with a wavelength of 1 to 100 cm) beyond the visible and thermal infrared region [2]. RADAR is classified as an active sensor [3]. RADAR sensing can obtain images regardless of it being day or night and in almost all weather conditions [4]. These advantages have been applied to visible/infrared radiation and passive sensors. Water clouds have a substantial effect on RADAR operating at wavelengths below 2 cm. The effects of rain are comparatively insignificant at wavelengths above 4 cm [2].

SAR is a microwave imaging system [5], in which SAR sensors acquire information from dissimilar backscattering mechanisms [6], transmitting signals of electromagnetic energy, and recording the responses returned from target surfaces [3]. For example, SAR operational flood detection relies on the physical response of water features when illuminated by the radar signal [6]: a smooth surface, such as a water body, causes specular reflection (the radar pulse is scattered away from the radar sensor) of the incident (side looking), and thus only a small intensity of energy is returned toward the radar. This results in the appearance of darker-toned areas on an image [7]. Generally speaking, the intensity of scene-generated variation in texture and tone

Manuscript received December 29, 2016; revised May 1, 2017.

Ponthip Limlahapun is with the Research fellow of the Japan Society for the Promotion of Science, Thailand (e-mail: thip.limlahapun@gmail.com)

H. Fukui is with the Chubu University, Japan.

depends on radar echoes from smooth or rough surfaces [8]. Radar backscatter increases with an increase in surface roughness [2], while water surfaces, regardless of external factors (i.e., wind causing waves) result in low backscattering, and other areas can be distinguished.

The first civilian SAR was operated by the US SEASAT in 1978 [2]. Major aerospace agencies launched and operated SAR sensors. For example, the Japan Aerospace Exploration Agency (JAXA) launched the Japanese Earth Resources Satellite (JERS) on February 11, 1992 followed by the Advanced Land Observing Satellite (ALOS), which carried an L-band active microwave sensor called a phased-array L-band synthetic aperture radar (PALSAR). Most recently, ALOS-2 was launched on May 24, 2014 [9]. In addition, the European Space Agency (ESA), which provides data for the European and African regions, launched the European Remote Sensing (ERS) satellites (ERS-1 and ERS-2), the Environmental Satellite (Envisat), and Sentinel-1 in 1991, 1995, 2002, and 2014 respectively (ESA) [10]. Other products include RADARSAT-1 and RADARSAT-2 (of the Canadian Space Agency, CSA) [11], TerraSAR-X (the first German national satellite) (Earth Observation Portal, 2015) [12], and the Constellation of Small Satellites for Mediterranean Basin Observation (COSMO-SkyMed) (of Italy), which offers radar data from a short revisit time [13]. Several active SAR products provide a selection of spatial resolutions, coverage areas, and observations of repeating cycles, which enable users to select an appropriate product based on their needs.

Applications of SAR imagery exist in various research areas. Examples include glacier movement detection [14], soil moisture measurement [15], and deforestation mapping [16]. Studies on hydrological and flood-related aspects of the design and implementation of SAR image processing and operation for flood-mapping retrieval also exist. Veljanovski et al., for example, investigated a suitable time series of radar images for mapping flood dynamics and ranges [17]. Flooding in urban areas was analyzed by Mason et al. with techniques of double scattering between the ground and buildings. This approach was proved to be efficient at detecting flooding in layover distortion regions [18]. An example of water information (wetness index and normalized difference vegetation index (NDVI)) extraction using radar and optical imagery (RADARSAT SAR and optical Landsat ETM+) was described in Wang et al. (2011) [19]. A high-resolution image (TerraSAR-X) using a fuzzy logic-based approach in which variables of a true value are applied in a degree range between 0 and 1 was proved to be an effective method for near-real-time flood detection [20]. In a subsequent study, Pulvirenti et al. detected inundated areas in multi-temporal COSMO-SkyMed data by searching for radar return signals using an automated image segmentation technique [13].

In addition, several papers have been presented in which SAR imagery was used for each observation capabilities and for addressing the need for flood-extent-based monitoring. Moreover, previous investigations have focused on specific products. For the present study, the black-and-white characteristic of SAR images enables visualization and interpretation of features contained in the image. This

requires considerable knowledge of the interaction mechanism between the microwave sensor and object. Therefore, development based on a detection algorithm to support various SAR products without requiring software installation is a challenge.

III. FRAMEWORK OF THE STUDY

This investigation did not focus on a specific area. Rather, the system was developed to detect inundated areas worldwide where Landsat and SAR imagery could be obtained. The SAR image detection algorithm was developed and tested with imagery downloaded from sample products distributed by data source provider (e.g., JAXA, ESA) websites. The Landsat dataset we used was downloaded from the US Geological Survey (USGS) website, where all of its archived data is freely accessible.

A. Data Source

The advanced synthetic aperture radar (ASAR), a sensor onboard the Envisat satellite, operates in the C band and can operate with the SAR image mode [21]. The archive data aids in monitoring of environmental and climatic changes obtained from 2002 to 2012. The mission officially ended on May 9, 2012 [10]. ASAR images were downloaded from the ESA website [21]. The imagery was acquired over Ecuador: one image represented a flood period in March 2008, while another was from September 2004 and was used for distinguishing flooded areas from permanent water features.

Sample scenes of PALSAR were downloaded from the Alaska Satellite Facility (ASF) [22] under academic purposes with an end user license agreement (EULA). Two of these scenes covered a northern part of Thailand. One image represented a dry season and the other represented a wet season acquired on December 2, 2007 and July 19, 2008, respectively. The other two images, one from January 9, 2007 in a dry season and the other from August 27, 2007 in a wet season, covered a central part of Cambodia where floods frequently occur. Both images were captured in the same acquisition mode and characteristics (fine beam, ascending, and off-nadir angles at 34.3 °) for minimizing the geometric distortions inherent in SAR acquisitions from different tracks [10].

The last two scenes of the ASAR wide swath medium (WSM) of a 150-m spatial resolution (150-m slant range x 150-m azimuth) covered Czech-Romania. The two images were obtained on April 4, 2006 and March 30, 2004 [10].

B. Approach

The system was composed of a background operating function and a frontier user interface.

Component 1: Operational Environment

These components were mainly for developing a browsing function and analysis algorithm, and for providing an inundated feature detection product to the user.

Data Handling: Imagery preparation in geo-reference tagged image file format (GEOTIFF) was performed. We experimented on a 64-bit Windows 7 PC with 8 GB of RAM. The image scenes downloaded from the original source provider had to be set with the maximum limit at

approximately 60 MB. For example, an ALOS PALSAR Cambodia image of 1GB was set to cover a 75 % area reduced to a volume of 0.6 GB. The new output file from this phase could not be otherwise created. The above-mentioned image size could be increased if memory was provided.

Algorithm and Image Processing: MATLAB was used as the prototyping backend environment. Users could not recognize the complex processing but could easily operate it through a web interface. The first adjustment was applied to the change of image numerical type (e.g., integer, floating point) to a double precision value. This function had no effect on the already proper image value. A trial and search for an appropriate mask threshold were implemented. However, products from different satellite tracks had no compromise value; therefore, few threshold values were selected to best suit the selected products. Filtering was applied to the resultant image of the previous step as the edge-enhancement operator. The next step applied structuring and a color assignment to the image for the outcome, which showed the inundated areas. The final product did not recognize the geo-referenced file; therefore, users had to select the header file that contained the data property and geographic location. This enabled the display in any web map service or GIS tool. Fig. 1 shows the detection inundated areas that were processed.

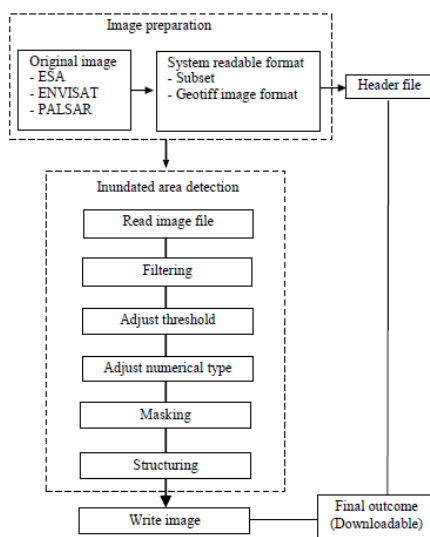


Fig. 1 Process assessment.

Component 2: Web Interface Environment

The interface was designed to reflect the above operation. The user must initially identify the selection of an image product source (e.g., PALSAR/JERS or ASAR). The platform to facilitate the image detection analysis was then implemented. This platform with other GIS dataset baselines (e.g., administrative boundaries, roads, rivers) was also included. Fig. 2 shows the detection diagram through web-based interface.

be identified by comparing pre- and post-imagery. By taking advantage of contextual information from the remote sensing data, the system helped support and simplify the processing of the image, such as a complex visualization scene (e.g., SAR). The analysis results of different products are discussed below.

PALSAR and ALOS-II products

The comparison results of the inundated areas detected by PALSAR with a fine-beam mode covered area in Cambodia and Sri Lanka are shown in Figs. 3 to 7.

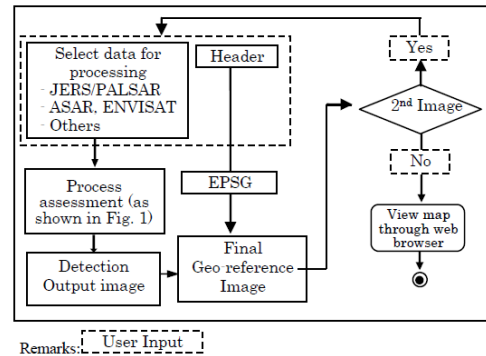


Fig. 2 Web interface manipulation.



Fig. 3. Reference map: overlay of a scene over world map.

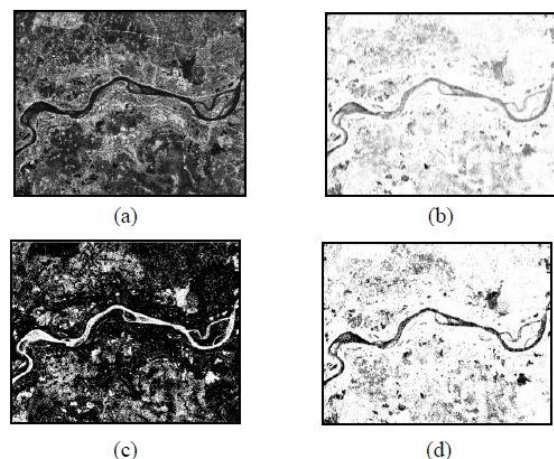


Fig. 4 Dry-season PALSAR image products of Cambodia January 9, 2007: (a) original, (b) filtered, (c) masked, and (d) final adjustment image (source original image: JAXA)

ENVISAT ASAR products

The non-orthorectified images over Ecuador were downloaded in original ASAR data format (*.N1). The NEXT free software provided by ESA [10] was used for the preparation process. There were two main components for preparing the images: an orthorectified image with a 90-meter (3 arc-second) DEM, which was a product acquired from the Shuttle Radar Topography Mission (SRTM) [1]; and a subset that was retained in the system in readable format Geotiff (Figs. 8 to 11).

IV. RESULTS

A. Image Analysis

A single inundated image could be detected from the remote sensing data. Flood investigation areas could possibly

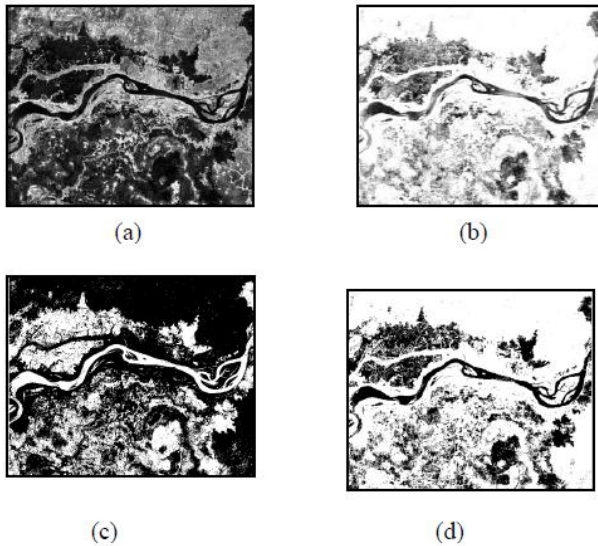


Fig. 5. Wet-season PALSAR image products, Cambodia August 27, 2007: (a) original, (b) filtered, (c) masked, and (d) final adjustment image (source original image: JAXA).

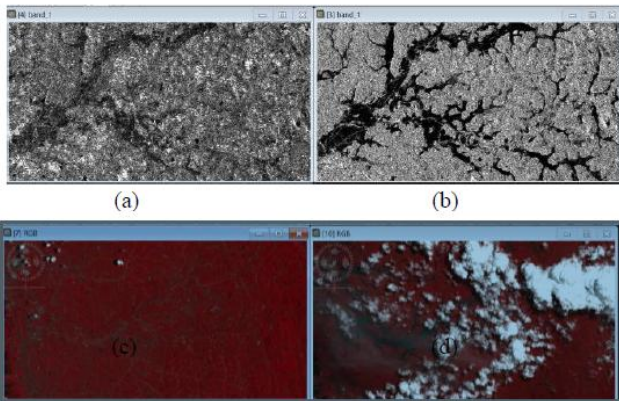


Fig. 6. Sri Lanka image products (a) ALOS-II, dry-season on February 3, 2016, (b) wet-season on May 16, 2016, (c) Landsat-8, dry-season on 31 March 2016, and (d) wet-season on 18 May, 2016 (source original image: ALOS: Sentinel Asia; Landsat: USGS).

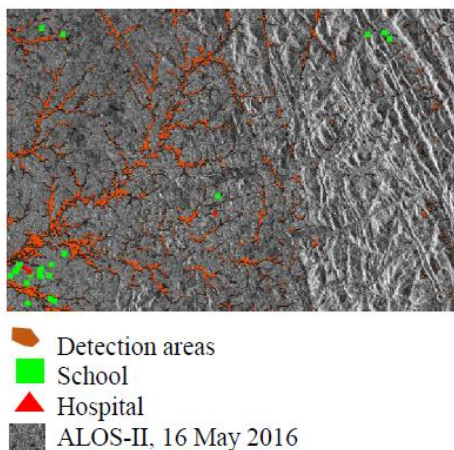


Fig. 7. Overlay of GIS dataset over detection areas (source image: JAXA, Sentinel Asia).

ERS-2 products

Similar to the above process, image products from ESA, Sentinel-1 and -2 were collected from the ESA, and ASF websites. Figs. 12 to 14 show the results of the image

processing.



Fig. 8. Reference map: overlay of an image scene over a world map (source image: ESA).

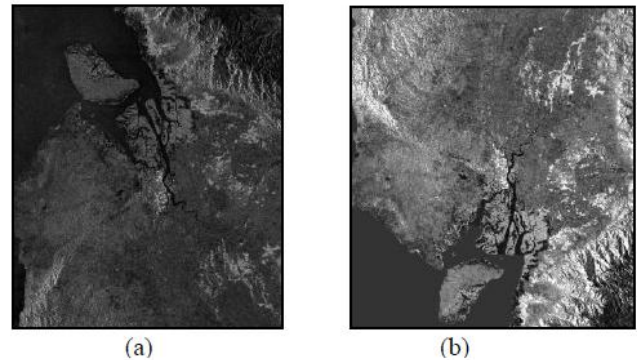


Fig. 9. ESA image products of Ecuador September 2, 2004: (a) original, (b) rectified.

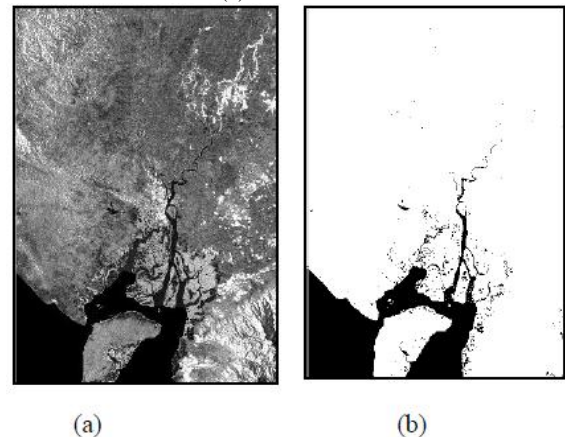


Fig. 10. Dry-season ESA image products of Ecuador September 2, 2004: (a) original, and (b) final adjustment (source original image: ENVISAT).

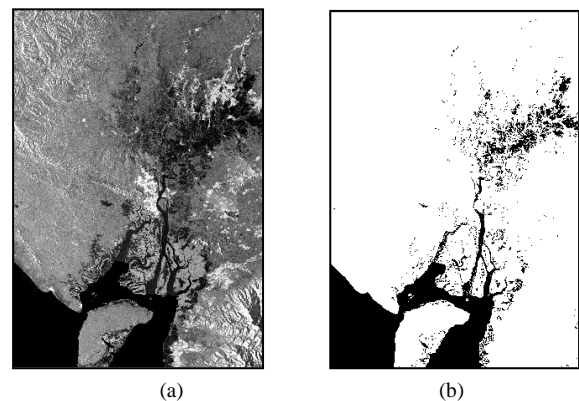


Fig. 11. Wet-season ESA image products of Ecuador, March 1, 2008: (a) original, and (b) final adjustment (source original image: ENVISAT)



Fig. 12. Reference map: overlay of an image scene over a world map (source image: ESA).

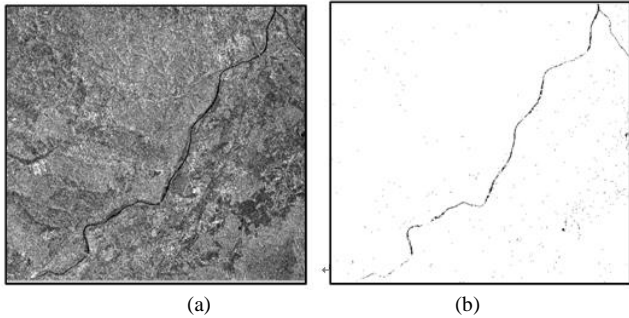


Fig. 13. Dry-season ERS-2 image products of southeastern Poland, August 12, 2009: (a) original, and (b) final adjustment (source: ERS).

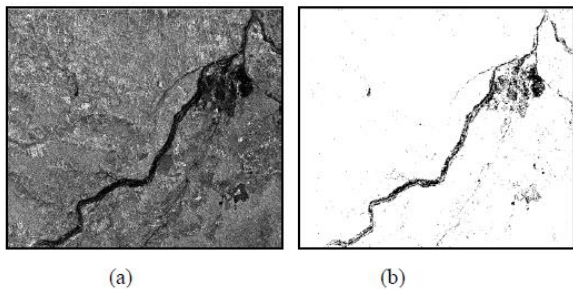


Fig. 14. Wet-season ERS-2 image products of southeastern Poland, May 19, 2010: (a) original, and (b) final adjustment (source: ERS).

B. Web-Based Manipulation Platform

The proposed system has some constraints in terms of operation speed on account of computing capacity and image format. On the other hand, its advantages are that it enables the user to operate and rapidly detect inundated areas in any location without the burden of software installation or manipulation for various SAR products.

Additionally, the system supports both Landsat and SAR imagery. In case of SAR, the user needs to specify products (i.e., PALSAR, Sentinel) to extract inundated areas. The process also requires header file and data information (i.e., datum, projections). These information could be acquired from the image providers and normally attached with data while downloaded. The user may extract and compare two images or downloaded the output in Geotiff format images. Inundated areas outcome can be seen in the viewer which will be automatically shown imageries before and after detection in the case of flooding. Web-based processed and outcome viewer are shown in Figs. 15 and 16, respectively.

Select image type you need to process

Select Image you have

Select Image you have

Landsat

SAR

Select Product Type

Select Product

Select Product

ERS SAR

ENVISAT ASA

PALSAR

SENTINEL

others

1st Sentinel SAR Image Detect Inundated Areas

subset_S1A_...1111_TC.tif

Input Header File

SAR 1st Image Header File Input (ex. Before Flooded Image) subset_S1A_...1111_TC.tif

Congratulations! Uploaded Reading file Successfully !

[Select Decimal Degree/UTM Zone](#)

Please Input Data Information to get EPSG Code

Datum Projection Zone Direction

You select WGS 84 Decimal Degree -----

[Process the 2nd PALSAR Image](#)

[Download 1st Detection Output](#)

[View Map](#)

Fig. 15. Web-based processed.

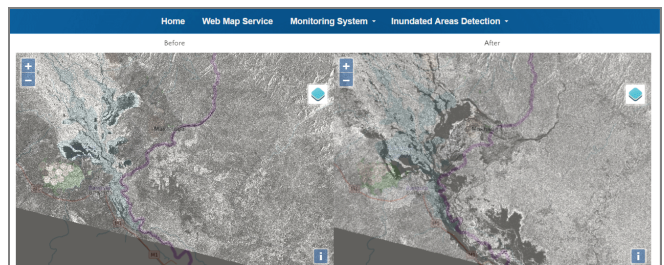


Fig. 16. Sentinel-2 image products of Malawi, Dry-season on November 11, 2014 (Left), and Wet-season January 22, 2015 (Right), (source: ASF [22]).

V. DISCUSSION AND CONCLUSION

Based on the results from using SAR images in various areas and different products, the inundated detection algorithm can be applied. The detected inundated areas can be used as guidelines for flood estimation. The outcomes of geo-referenced images can be converted to spatially superimposed using GIS software tools. Despite some limitations that may affect processing time (e.g., image size, format), the proposed evacuation plans (e.g., routes, shelters) and in flood response and recovery plans.

The findings showed that the proposed method of determining flooded areas using web-feature-based could be implemented to investigate flooding areas more rapidly and uncomplicated. We developed a tool for aftermath flood

mapping that used a web-based interface. Use of SAR imagery is encouraged as a spatial-based flood damage assessment in emergency situations and observation contributions where useable optical images are lacking. Therefore, disaster management requires a constellation of satellites in different sensor products on account of a single type that may lack coverage in the area of interest. This paper highlighted a tool that supports and operates various sensor capabilities and enables a simpler interpretation and visualization than image processing software. The results show that the proposed algorithm can be used to generate interactive inundation maps from SAR imagery of different satellite missions for visualization and comparison before and after flood events.

ACKNOWLEDGMENT

This project and publication were funded by the Japan Society for the Promotion of Science (JSPS) under a Postdoctoral Fellowships for Overseas Researchers and Grants-in-Aid for Scientific Research (KAKENHI) grant. Any opinions, findings, and conclusions expressed in this publication are those of the authors and do not necessarily reflect the views of the JSPS.

REFERENCES

[1] National Aeronautics and Space Agency (NASA). [Online]. Available: <http://ls7pm3.gsfc.nasa.gov>

[2] F. M. Henderson and A. J. Lewis, "Principles and applications of imaging radar," *Manual of Remote Sensing*, Third Edition, vol. 2, 1998.

[3] J. R. Jensen, "Introductory digital image processing, A remote sensing perspective," 4th Edition, Upper Saddle River, NJ, Prentice-Hall, Inc., 2016.

[4] M. Simons and P. A. Rosen, "Interferometric synthetic aperture radar geodesy," *Treatise on Geophysics-Geodesy*, vol. 3, pp. 339-385, 2007.

[5] S. C. Liew, "Remote sensing tutorial, center for remote imaging," *Sensing and Processing (CRISP)*, National University of Singapore, 2001.

[6] S. Stian and S. Inger, "Towards operational flood mapping with satellite SAR," in *Proc. the 2004 Envisat & ERS Symposium (ESA SP-572)*, April 2005.

[7] National Resources Canada. Target interaction and image appearance. [Online]. Available: <http://www.nrcan.gc.ca/earth-sciences/geomatics/satellite-imagery-air-photos/satellite-imagery-products/educational-resources/9311>

[8] T. Y. Gan, F. Zunic, C. C. Kuo, and T. Strobl, "Flood mapping of Danube river at Romania using single and multi-data ERS2-SAR images," *International Journal of Applied Earth Observation and Geoinformation*, vol. 18, pp. 69-81, August 2012.

[9] Japan aerospace exploration agency (JAXA). [Online]. Available: <http://global.jaxa.jp/>

[10] European space agency (ESA). [Online]. Available: <https://earth.esa.int/>

[11] Canadian space agency (CSA). [Online]. Available: <http://www.asc-csa.gc.ca/eng/satellites/>

[12] Earth observation portal. [Online]. Available: <https://directory.eoportal.org/web/eoportal/satellite-missions/t/tersasar-x>

[13] L. Pulvirenti, M. Chini, N. Pierdicca, L. Guerriero, and P. Ferrazzoli, "Flood monitoring using multi-temporal COSMO-SkyMed data: Image segmentation and signature interpretation," *Remote Sensing of Environment*, vol. 115, issue 4, pp. 990-1002, April 2011.

[14] J. Li, Z. Li, X. Ding, Q. Wang, J. Zhu, and C. C. Wang, "Investigating mountain glacier motion with the method of SAR intensity-tracking: Removal of topographic effects and analysis of the dynamic patterns," *Earth-Science Reviews*, vol. 138, pp. 179-195, November 2014.

[15] G. Bertoldi, S. D. Chiesa, C. Notarnicola, L. Pasolli, G. Niedrist, and U. Tappener, "Estimation of soil moisture patterns in mountain grasslands by means of SAR RADARSAT2 images and hydrological modelling," *Journal of Hydrology*, vol. 516, pp. 245-257, August 2014.

[16] S. S. Saatchi, J. V. Soares, and D. S. Alves, "Mapping deforestation and land use in amazon rainforest by using SIR-C imagery," *Remote Sensing of Environment*, vol. 59, issue 2, pp. 191-202, February 1997.

[17] T. Veljanovski, P. Pehani, and K. Ostir, "Comparison of three techniques for detection flooded areas on ENVISAT and RADARSAT-2 satellite image," *Geoinformation for Disaster Management*, vol. 29, no. 9, September 2011.

[18] D. C. Mason, L. Giustarini, J. G. Pintado, and H. L. Cloke, "Detection of flooded urban areas in high resolution Synthetic Aperture Radar images using double scattering," *International Journal of Applied Earth Observation and Geoinformation*, vol. 28, pp. 150-159, May 2014.

[19] Y. Wang, R. Ruan, Y. She, and M. Yan, "Extraction of Water Information based on Radarsat SAR and Landsat ETM+," *Procedia Environmental Sciences*, vol. 10, part C, pp. 2301-2306, September 2011.

[20] S. Martinis, J. Kersten, and A. Twele, "A fully automated TerraSAR-X based flood service," *ISPRS Journal of Photogrammetry and Remote Sensing*, vol. 104, pp. 203-212, June 2015.

[21] C. Stewart. Flood mapping with next ESA SAR Toolbox (NEST). [Online]. Available: <https://earth.esa.int/web/nest/home>

[22] Alaska Satellite Facility (ASF). [Online]. Available: <https://vertex.daac.asf.alaska.edu>



P. Limlahapun obtained her B.S. degree from Thammasat University, Bangkok, Thailand in 1994. She received the master of arts in geography at the Western Michigan University in 2002. She received the doctor of philosophy degree in media and governance from Keio University in 2011.

Her research interests include database management, water-related disaster issues and Geography Information System and Remote

Sensing applications for sustainable development.

In 2002-2007 and 2013-2014, she worked at the Geoinformatics Center, Asian Institute of Technology, Thailand as a researcher in the field of an Interactive GIS, database and project management. At present, she is a research fellow of Japan Society for the Promotion of Science hosted by International Digital Earth Applied Science Research Center at Chubu University.



H. Fukui He graduated from Nagoya University in 1980. He received the doctor of science degree in Earth sciences from Nagoya University in 1987. He is a professor of Chubu University and serves as the director of International Digital Earth Applied Science Research Center (IDEAS) of Chubu Institute for Advanced Studies in natural disasters from April, 2011. Before joining Chubu University, he was as a Professor of the Faculty of

Policy Management of Keio University.

His current research interests include regional planning, ecological development, global environment issues and education for sustainable development from the view point of spatial information sciences.

He has served on secretary general of GIS Association Japan, on Board of Directors in International Society for Digital Earth, Center for Environment Information Sciences, and as an adjunct professor of Chinese Academy of Sciences.